



HAL
open science

4MOST Low Resolution Spectrograph MAIT

Florence Laurent, Didier Boudon, Patrick Caillier, Diane Chapuis, Eric Daguisé, Karen Disseau, Aurélien Jarno, Jean-Emmanuel Migniau, Arlette Pécontal-Rousset, Alban Remillieux, et al.

► **To cite this version:**

Florence Laurent, Didier Boudon, Patrick Caillier, Diane Chapuis, Eric Daguisé, et al.. 4MOST Low Resolution Spectrograph MAIT. Ground-based and Airborne Instrumentation for Astronomy VIII, Dec 2020, Online Only, France. pp.188, 10.1117/12.2561487 . hal-04785314

HAL Id: hal-04785314

<https://hal.science/hal-04785314v1>

Submitted on 15 Nov 2024

HAL is a multi-disciplinary open access archive for the deposit and dissemination of scientific research documents, whether they are published or not. The documents may come from teaching and research institutions in France or abroad, or from public or private research centers.

L'archive ouverte pluridisciplinaire **HAL**, est destinée au dépôt et à la diffusion de documents scientifiques de niveau recherche, publiés ou non, émanant des établissements d'enseignement et de recherche français ou étrangers, des laboratoires publics ou privés.

4MOST Low Resolution Spectrograph MAIT

F. Laurent^{*a}, Didier Boudon^a, Patrick Caillier^{a,c}, Diane Chapuis^a, Eric Daguise^a, Karen Disseau^a, Aurélien Jarno^a, Jean-Emmanuel Migniau^a, Arlette Pécontal^a, Alban Remillieux^a, Johan Richard^a

^aUniv Lyon, Univ Lyon1, Ens de Lyon, CNRS, Centre de Recherche Astrophysique de Lyon UMR5574, F-69230, Saint-Genis-Laval, France ;

^bESO, Karl-Schwarzschild-Str. 2, D-85748 Garching bei München, Germany

ABSTRACT

4MOST, the 4m Multi Object Spectroscopic Telescope, is an upcoming optical, fibre-fed, MOS facility for the VISTA telescope at ESO's Paranal Observatory in Chile. Its main science drivers are in the fields of galactic archeology, high-energy physics, galaxy evolution and cosmology. The design of 4MOST features 2436 fibres split into low-resolution (1624 fibres, 370-950 nm, $R > 4000$) and high-resolution spectrographs (812 fibres, three arms, ~ 44 -69 nm coverage each, $R > 18000$) with a fibre positioner and covering a hexagonal field of view of ~ 4.1 deg². The 4MOST consortium consists of several institutes in Europe and Australia under leadership of the Leibniz-Institut für Astrophysik Potsdam (AIP). 4MOST is currently in its Manufacturing, Assembly, Integration and Tests Phase with an expected start of science operations in 2022.

Two third of the fibers (i.e. 1624 for science and 20 for calibration) feed the two Low Resolution Spectrographs hosting three channels each. The fibers used are 85 μ m core fibers at $f/3$. Each Low Resolution Spectrograph is composed of a 200mm beam for an off-axis collimator associated to its Schmidt corrector, 3 "color" arms with $f/1.73$ cameras and standard 6k x 6k 15 μ m pixel detectors. CRAL has the global responsibility of the Low Resolution Spectrographs.

In May 2018, the final design review for the 4MOST Low Resolution Spectrograph was passed successfully. In this paper, the long process from the definition of the technical requirements for all individual opto-mechanical components, the manufacturing, the deliveries up to the first assemblies will be described.

Keywords: 4MOST, VISTA, ESO, Spectrograph, Design, Performances, MAIT

1. INTRODUCTION

4MOST is a wide-field, high-multiplex spectroscopic survey facility under development for the VISTA telescope of the European Southern Observatory (ESO). Its main science drivers are in the fields of galactic archeology, high-energy physics, galaxy evolution and cosmology [1]. 4MOST will in particular provide the spectroscopic complements to the large area surveys coming from space missions like Gaia, eROSITA and Euclid, and from ground-based facilities like VST, DESI, LSST and SKA. The VISTA Wide Field Corrector design provides a focal surface at the conventional Cassegrain focus [2]. 4MOST features a 4.1 degree diameter field-of-view with 2436 fibres in the focal plane that are configured by a fibre positioner based on the tilting spine principle [3]. The fibres feed two types of spectrographs; 1624 fibres go to two spectrographs with low resolution $R > 4000$ and 812 fibres to a high resolution spectrograph with $R > 18,000$ [4]. Both types of spectrographs are fixed-configuration, three-channel spectrographs. 4MOST will have a unique operation concept in which 5 years public surveys from both the consortium and the ESO community will be combined and observed in parallel during each exposure, resulting in more than 25 million spectra of targets spread over a large fraction of the southern sky [5].

*florence.laurent@univ-lyon1.fr; phone +33 4 78 86 85 33; <http://cral.univ-lyon1.fr/>

This paper will focus on the LRS MAIT which is under CRAL responsibility. The LRS is driven by providing a high spectral resolution over a large spectral range. Section 2 of this paper introduces the LRS design and key requirements. Section 3 summarizes the approach for MAIT analysis. The manufacturing of optical and mechanical components is presented in sections 4 and 5. The technical requirements for each individual opto-mechanical component is described. Finally, section 6 compiles the conclusions and future developments.

2. 4MOST LRS DESIGN AND KEY REQUIREMENTS

The LRS is composed of two symmetrical unit spectrographs including the same optical components. Each unitary spectrograph should meet the key requirements listed hereafter. Each spectrograph is fed by an entrance slit of 812 science fibres. After collimation, the optical beam is separated in three spectral bandwidths, dispersed and reimaged in three different channels with F/1.73 aperture. The separation in three channels provides the minimal resolution of 4000 (Figure 1). The Blue arm goes from 370 to 554 nm, the Green from 524 to 721 nm and the Red from 691 to 950 nm.

The LRS is composed of the 7 following sub-assemblies:

- An Entrance Slit Unit (ESU) composed of 812 science fibres following focal plane curvature radius. A Slit Field Lens is glued onto the entrance slit
- A mirror acts as a Collimator collecting the F/3 light from the fibres and generates a collimated beam of 200mm.
- A Dichroic: Dichroic beam splitters in front of the Schmidt corrector separate the three channels. There are two dichroics (Red and Blue).
- In addition, each channel includes a corrector, a VPHG for dispersion, a dioptric camera and a Field Lens Window. The spectral overlap of the channels is determined by the edge of the dichroic and here assumed to be 30nm. A 6k x 6k detector with 15microns/pixel records the spectra.

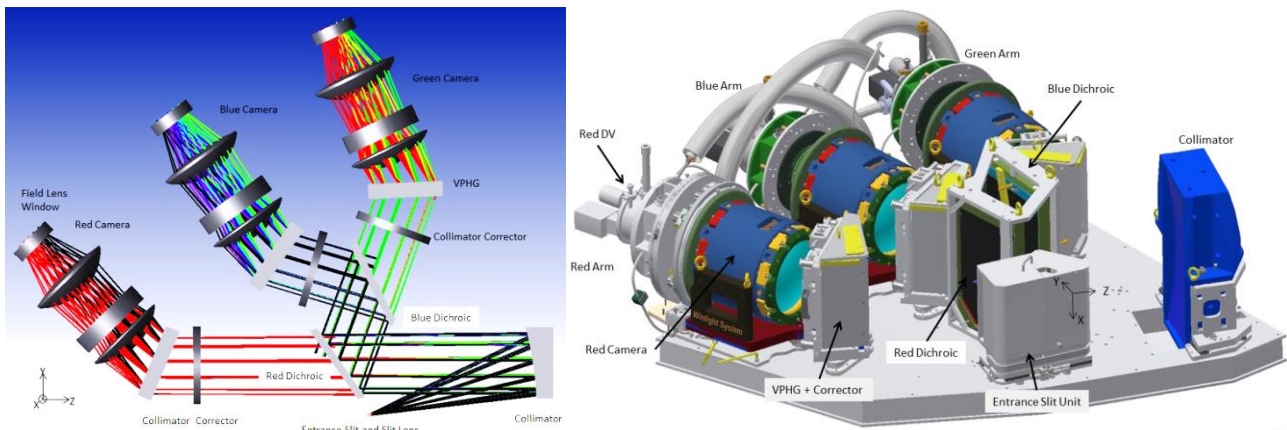


Figure 1: Left: LRS optical layout. Right: LRS mechanical model

The LRS key design requirements are derived from the 4MOST top level requirements ([6] and [7]) and are listed below:

1. The LRS shall be able to accommodate a minimum of 812 science fibres and 10 calibration fibres. It shall accept f/3.0, with 85 micron core diameter fibre inputs. The LRS shall cover simultaneously the wavelength range from 400 nm to 885 nm (goal: from 370 nm to 950 nm). The LRS spectra shall be projected on 6k by 6k, 15 micron pixel detector(s).
2. The LRS spectral resolving power shall be:
 - $R \geq 10 \times \lambda/\text{nm}$ for $400 \text{ nm} \leq \lambda < 500 \text{ nm}$, and
 - $R \geq 5000$ for $500 \text{ nm} \leq \lambda \leq 885 \text{ nm}$.
3. The LRS spectral sampling shall be ≥ 2.5 pixel (goal 3.0 pixels).

3. APPROACH FOR MAIT ANALYSIS

3.1 Budget repartition for image quality

The image quality of the LRS is the main requirement for 4MOST. It is directly related to the FWHM spectral sampling and spectral resolving power requirements. No requirements onto Gaussian FWHM PSF or RMS Spot Radius or Ensquared Energy are given. Unfortunately, these last data are often used when an optical layout is designed with Zemax. A first study consists in finding an equivalence between fibre image FWHM and Gaussian FWHM PSF or RMS Spot Radius or Ensquared Energy - Table 1. To reach 5000 in spectral resolving power, the average maximal spectral sampling in FWHM is 3.1 pixels. Taking into account a PSF approximation as a Gaussian, the convolution of Gaussian PSF and fibre image gives the real image onto the CCD. With that, and simulations in Zemax, the maximal spectral sampling in FWHM of 3.1 pixels is equivalent to the numbers provided in Table 1. To faster the analysis in Zemax, we decide to work with RMS Spot Radius rather than ensquared energy or PSF.

The total budget in image quality is shared in 5 parts, the quadratic sum of which should stay within the main system budget. The initial budget is divided in percentage as presented in Figure 2 for average values. The design represents 80% of the budget for image quality. For the manufacturing, alignment, environment and margins, a 30% degradation of the RMS spot radius is allocated for each part.

Table 1: Equivalence between maximal spectral sampling in FWHM of 3.1pixels with Gaussian FWHM PSF / RMS Spot radius / 95% of Ensquared Energy

	Maximal Spectral Sampling in FWHM of 3.1pixels is equivalent to	
	Maximal	Average
Gaussian FWHM PSF (μm)	34.0	23.0
RMS Spot radius (μm)	20.25	13.9
95% of Ensquared Energy (μm^2)	56.5	38.5

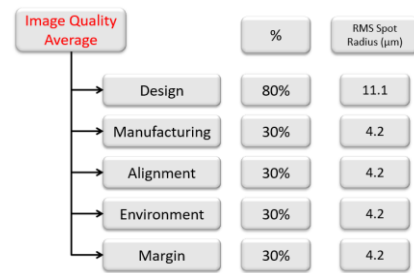


Figure 2: Initial Budget for image quality for average values

3.2 Sensibility

The alignment sensitivity analysis is done using Zemax. The approach to the analysis is as follows:

- Beginning with the nominal LRS optical design, each optical group is individually perturbed by a prescribed amount in each degree of freedom (DOF). For most groups, the perturbations that are modeled are lateral displacement (x, y), angular rotation ($\theta_x, \theta_y, \theta_z$), and longitudinal displacement (z).
- The sensitivity analysis is performed onto 12 optical groups (Slit, Entrance Slit, Slit Field Lens, Collimator, Dichroic Red and Blue, Corrector, VPHG, Camera (composed of 3 lenses), Field Lens Window (FLW), CCD and Detector Vessel – DV (composed of Field Lens Window and CCD).
- Two changes in the system are evaluated onto the CCD plane at central wavelength for each arm:
 - The RMS spot radius (RSCE) degradation (Average of 9 FoV onto 5 wavelengths that means 45 data). Note that the RMS spot radius is the most important requirement for the analysis,
 - The image shift along x and y -axes (shift of 4 FoV corresponding to the 4 CCD corners are averaged).
- Dividing the change in the RSCE/image shift by the magnitude of the perturbation yields the sensitivity for that optic in that DOF.
- The sensitivity for each optic is then multiplied by the tolerance assigned to that optic for that DOF.
- A table is then created, listing the sensitivities of each optic, and their prescribed tolerances in each DOF (Table 2). The results are summed in rms, and the total is entered into the LRS system budget to check the compliance with the top-level requirements.

3.3 Tolerancing approach for manufacturing

The tolerancing analysis is performed on each optical component individually. It takes into account manufacturing errors on optical components ie. the incorrect radius of curvature, glass thickness, surface shape, curvature center offset from

mechanical centre, index accuracy and abbe number. This study is performed to set the individual technical requirements for the optical suppliers.

For each optical component, the tolerancing analysis is performed according to the three main criteria:

- The image quality degradation: The rms spot radius degradation should be lower than 10%. The 10% is directly derived from the budget repartition detailed in Figure 2. There are 12 optical components as explained in section 3.2. The quadratic sum for the image quality degradation for these 12 optical components is equivalent to a degradation of 4.2 microns as mentioned in Figure 2.
- The image shift: The image shift should be lower than 1.5 CCD pixels.
- The vignetting: No vignetting should occur.

Note that the tolerancing is done only on the image quality criterion. The image shift and vignetting are only checked at the end of the tolerancing.

3.4 Tolerancing approach for alignment

The tolerancing analysis is performed for alignment errors onto the 12 elements defined in the sensitivity analysis. This study is performed to define the adjustment elements onto the mechanical design.

The tolerancing analysis is performed according to the 3 main criteria:

- The image quality degradation: The rms spot radius degradation should be lower than 4.2µm. The 4.2 microns is derived directly from the budget repartition detailed in Figure 2.
- The image shift: The image shift should be lower than 5 CCD pixels.
- The vignetting: No vignetting should occur.

First, the tolerancing analysis is performed onto blue arm without compensator. The Table 2 gives the tolerances to reach image quality and image shift requirements. The nominal tolerances ($\pm 0.5\text{mm} / \pm 5\text{arcmin}$) are relevant. The introduction of compensators is mandatory due to tight tolerances done by tolerance analysis without compensator.

Second, to reach image quality and image shift requirements, the following adjustments are set: the entrance slit as reference, the Collimator in (x, y), the Dichroics in (θ_x, θ_y), the VPHG in (θ_z), the Camera in (θ_x, θ_y) and the DV in (x, θ_x, θ_y). All other degrees of freedom are set at the nominal positioning ($\pm 0.5\text{mm} / \pm 5\text{arcmin}$).

The main contributors for the image shift are the Collimator [(θ_x, θ_y) or (x, y)], the Dichroics (θ_x, θ_y), the Camera [(θ_x, θ_y) or (x, y)], the DV (x, y) and CCD (x, y). The main contributors for the spot radius degradation are the Camera (z), DV (z), CCD (z) and the Collimator [(θ_x, θ_y) or (x, y)].

Table 2: Left: Tolerances to reach image quality and image shift requirements (in red the more stringent tolerances). Right: Foreseen adjustments

	X (µm)	Y (µm)	Z(µm)	Tx (arcsec)	Ty (arcsec)	Tz (arcsec)		X (µm)	Y (µm)	Z(µm)	Tx (arcsec)	Ty (arcsec)	Tz (arcsec)
Slit	63	63	51	299	173	150	Slit						
Slit Field lens	500	500	500	299	299	299	Slit Field lens						
Slit+Slit Field lens	63	63	50	60	166	75	[Slit+Slit Field lens]			Home made stage			
Coll Mirror	63	63	50	9	9	75	Coll Mirror	Shimming	Home made stage				
Dichro_Red	500	500	258	9	9	299	Dichro_Red				Home made stage	Home made stage	
Dichro_Blue	500	500	250	9	9	299	Dichro_Blue				Home made stage	Home made stage	
Corrector	500	262	500	299	299	299	VPHG						Home made stage
VPHG	500	500	500	299	299	19	Camera+DV				Home made stage	Home made stage	
Camera+DV	500	500	500	19	19	150	Camera						
Camera	31	31	16	37	37	299	DV			Motorized home made stage	Home made stage	Home made stage	
DV	31	31	16	78	79	150	FLW						
FLW	128	98	66	229	299	299	CCD						
CCD	31	31	16	118	152	150							

3.5 Budget repartition for alignment

For each component, the global budget ($\pm 0.5 \text{ mm}$ in X, Y, Z and $\pm 5 \text{ arcmin}$ in $\theta_X, \theta_Y, \theta_Z$) is shared in these 2 main levels and additional level for adjustment and margins as presented in Figure 4.

The components proper positioning and alignment are ensured by 2 main levels of tolerancing:

- The first level is done on Mounted Optical Bench wrt PLP Interface. Each optical component will be interfaced with the optical bench through a kinematic mount ensuring precise and reproducible positioning shown in Figure 3.
- The second level is done on PLP Interface wrt Mechanical components reference & Mechanical components reference wrt Optical components reference. That corresponds between the kinematic interface and the optical components reference surface.

This global budget and repartition is clearly optimistic due to quasi arithmetic sum of tolerancing errors. Due to tolerancing error statistical distribution, a RMS approach also can be applied, giving relaxed values.

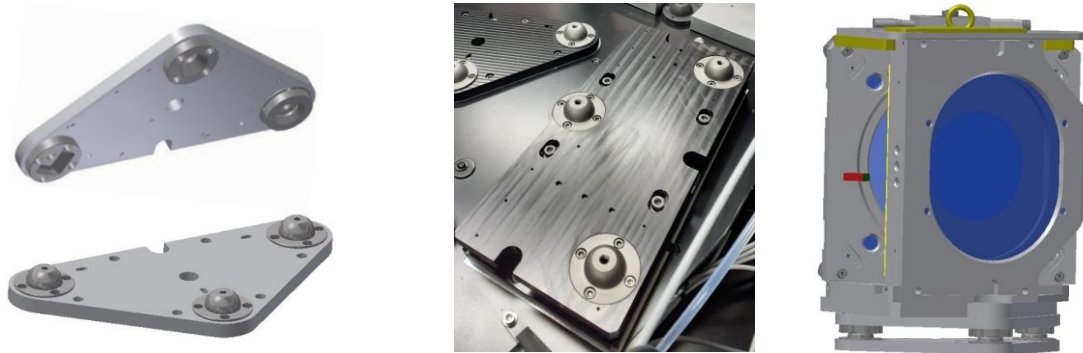


Figure 3: Kinematic mounting example. Left&Middle: Without assemblies. Right: With dispersive assembly

Global Alignment Budget						
	x (\pm mm)	y (\pm mm)	z (\pm mm)	θ_x (\pm arcmin)	θ_y (\pm arcmin)	θ_z (\pm arcmin)
Requirements	0.50	0.50	0.50	5.0	5.0	5.0
Mounted Optical Bench wrt PLP Interface	0.25	0.25	0.25	2.5	2.5	2.5
PLP Interface wrt Mechanical components reference & Mechanical components reference wrt Optical components reference	0.25	0.25	0.25	2.5	2.5	2.5
Adjustable components	0.05	0.05	0.05	0.5	0.5	0.5
Margins	0.05	0.05	0.05	0.5	0.5	0.5

Figure 4: Global alignment budget and repartition

For the measurements of optical components wrt global reference, there are different levels of measurements:

- For the supplier, the optical surfaces have been specified wrt Optical components reference (mainly the optic edges). The test report will be provided by the supplier.
- The Mechanical components reference will be measured wrt PLP interface either by CRAL or by the mechanical supplier
- The optical component is integrated into its mechanics
- The PLP interface is measured with the Hexagon arm - Figure 5, Left
- After integration, the Optical components reference will be measured through the holes by probing the optic edges wrt PLP interface. Each barrel has “holes” in order to directly probe the Optical component reference which is the supplier reference - Figure 5, Right.

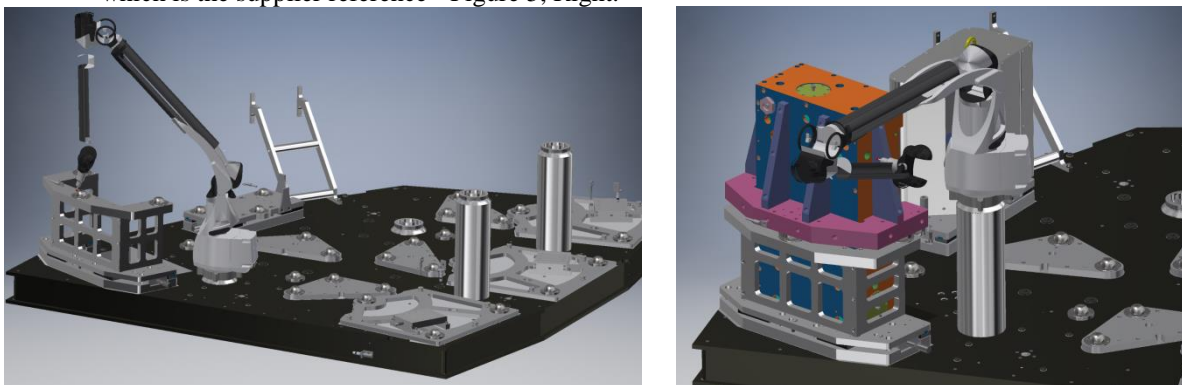


Figure 5: Measurement with the Hexagon arm. Left: PLP interface. Right: Optical components reference

4. OPTICAL COMPONENTS MANUFACTURING

All optical components are specified with a H3 refractive index homogeneity in accordance with ISO standard 10110, striae grade of glass A per MIL-G-174B standard, stress birefringence of glass better than 10nm/cm and bubble classification of glass 1 class (DIN 58927). A residual surface roughness of 3nm rms over the clear aperture is required. According to MIL-PRF-13830B specification (superseding MIL-O-13830), the surface imperfections of each optical surface shall be less than 60/40. The coating is required onto clear aperture for angle of incidence on useful wavelength range. The effect of the irregularity of each optical surface comes from optical surface itself and its coating. The components shall be designed for lifetime, operation, test, storage and survival conditions.

4.1 Collimator

The collimator size is a rectangle of 580x260mm² with an on-axis center thickness of 80mm. The manufacturing tolerances of the optical surface wrt mechanical interface are expected to be of ± 0.05 mm X, Y, ± 0.1 mm Z, ± 0.5 arcmin θ_X , θ_Y and ± 1.5 arcmin θ_Z . It is made of fused silica with a curvature radii of 1200mm \pm 0.3%. The irregularity shall be lower than 0.1 lambda rms. The average reflectivity shall be higher than 97.5% with a minimum at 95%. Winlight System, Fr has manufactured the collimator and proceeded to its integration in its mount, provided by Almeras, Fr. The optical part is mounted in kinematic way to avoid any stress or deformation. As identified in the global alignment Table 2, the Collimator mirror includes a translation function for Y adjustment. The X adjustment is done by shimming at the level of the kinematic mount.

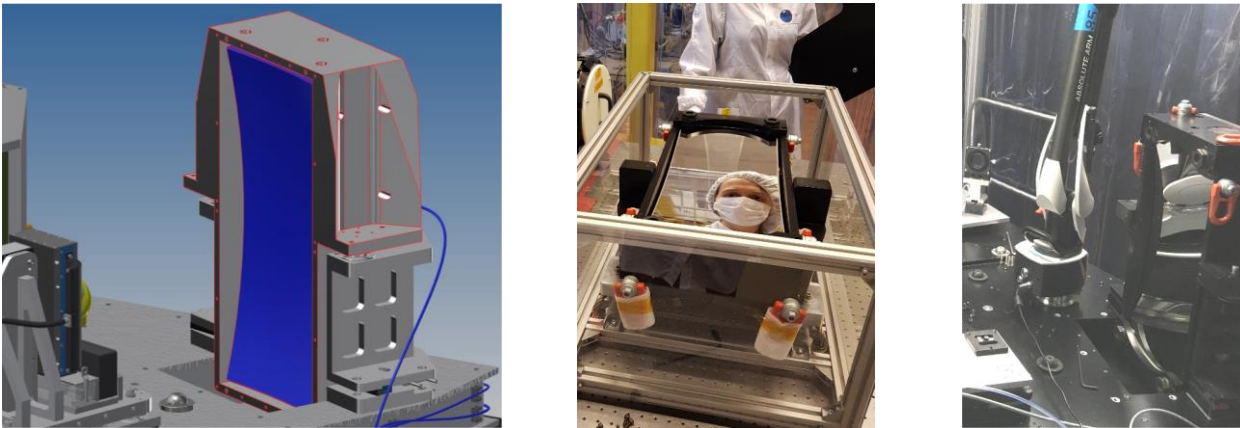


Figure 6: LRS Collimator: Design and manufacturing

4.2 Dichroic

The Red Dichroic shall reflect wavelength in the blue range (from 370 nm to 691 nm) and transmit the red range (from 721 nm to 950 nm). The Blue Dichroic shall reflect wavelength in the blue range (from 370 nm to 524 nm) and transmit the red range (from 554 nm to 721 nm). The manufacturing process performed by LMA, Fr is described in the paper [8]. The main requirements on the dichroics is the coating.

The front face of Red Dichroic shall be dichroic coated ensuring:

- Average reflectivity over 97% and minimum reflectivity of 92% from 370 nm to 691 nm
- Average transmission over 98% and minimum transmission of 95% from 721 nm to 950 nm

The front face of Blue Dichroic shall be dichroic coated ensuring:

- Average reflectivity over 97% and minimum reflectivity of 92% from 370 nm to 524 nm
- Average transmission over 98% and minimum transmission of 95% from 554 nm to 721 nm

The rear face of both dichroics shall be AR coated. The AR coating transmission shall be over 99% on wavelength range.

The transition profile shall be:

- Nominal transition wavelength is 706 nm \pm 7nm for Red Dichroic and 539 nm \pm 5nm for Blue Dichroic
- A transition from reflection to transmission is required. Transition shall be < 30 nm from 95%R to 5%R.

The Angle of Incidence of Red respectively Blue dichroic is of $35.35^\circ \pm 1^\circ$ respectively $43.58^\circ \pm 1^\circ$. The irregularity on the front face (reflected surface) shall be lower than $< 0.2\lambda$ rms at 633nm; on the back face (transmitted surface) shall be less than 0.4λ rms.

Both dichroics are integrated in a common mount (manufactured by Gami, Fr) in order to limit the number of interfaces with the bench in a much-crowded area and also to increase the overall rigidity of the mount. In conformance with the global alignment Table 2, the Dichroics are adjustable in θ_X and θ_Y orientation. They are also mounted in a kinematic way. As shown hereafter, the mount is also particularly constrained by the optical beam.

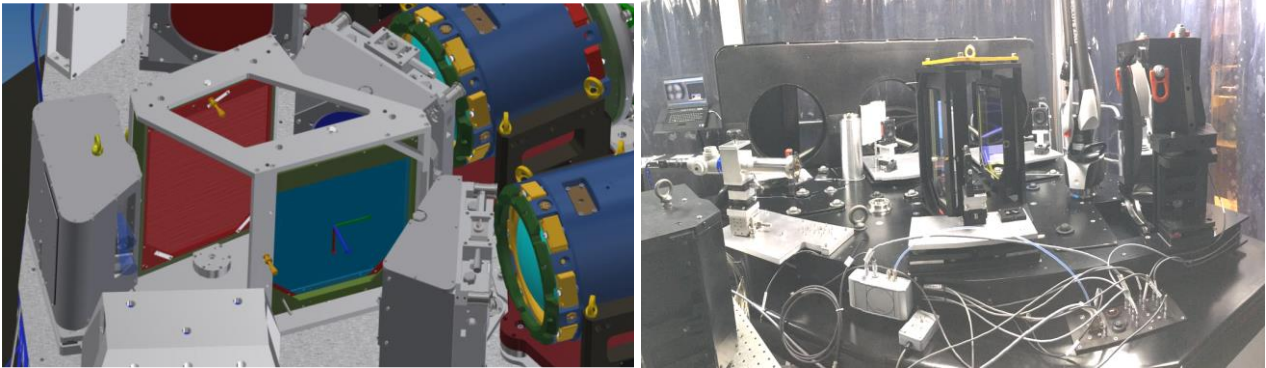


Figure 7: LRS dichroics: Design and manufacturing

4.3 Corrector

The corrector is manufactured and integrated in its mount by Winlight System, Fr. Its size is a diameter of 275mm with an on-axis center thickness of $25 \pm 0.1\text{mm}$. That is a plano-parallel plate with one off-axis aspheric onto rear surface made of fused silica. The off-axis is $170\text{mm} \pm 0.2\text{mm}$. The aspheric coefficients of each corrector are different for each arm. The manufacturing tolerances of the optical surface wrt mechanical interface are expected to be of $\pm 0.05\text{ mm X, Y, } \pm 0.1\text{ mm Z, } \pm 0.5\text{ arcmin } \theta_X, \theta_Y$ and $\pm 2\text{ arcmin } \theta_Z$. For plane surface, ± 10 fringes @ $\lambda=633\text{ nm}$ is accepted for the power. The effect of the irregularity shall be lower than $0.05\lambda\text{ rms}$. The average AR coating shall be lower than 1% with a minimum at 2%.

In a similar way and for similar reasons as for the dichroics, the Correctors, VPHG and pupil mask are mounted together in a common mount called “dispersive assembly” and manufactured by Almeras, Fr. For the Correctors no alignment is identified in the global alignment Table 2.

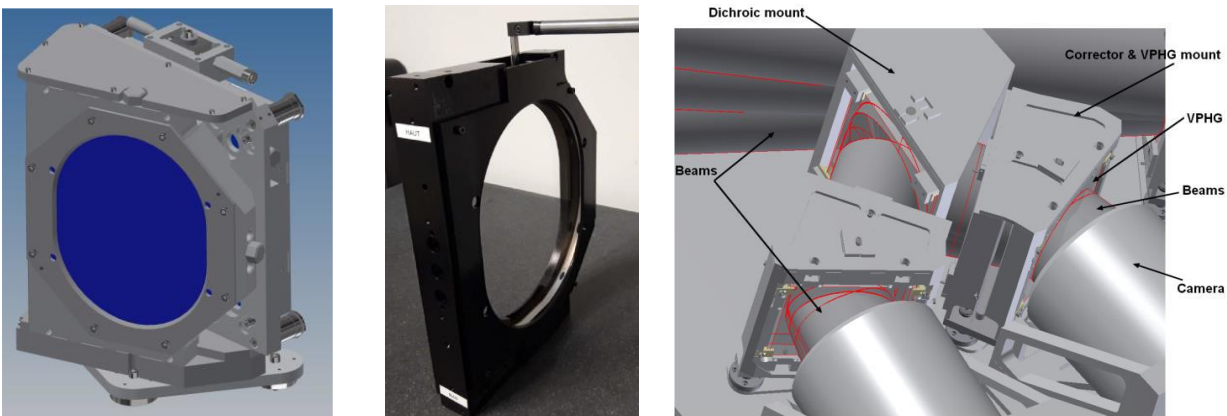


Figure 8: LRS Corrector: Design and manufacturing

4.4 VPHG

The 6 VPHGs are manufactured by Wasatch Photonics, USA. Each VPHG works in transmission, on the +1 order of diffraction with unpolarised light. Each VPHG is made of 3 elements:

- A Entrance coated grating plate: AR coated only single side,
- The holographic gelatin and associated bounding,
- A Closing coated grating plate: AR coated only single side.

The Blue/Green/Red VPHG is used at incidence angle of $18.65^\circ / 22.68^\circ / 22.65^\circ \pm 1.00^\circ$. The Blue/Green/Red VPHG has a lines frequency of $1351 / 1220 / 925 \pm 1$ lines/mm. The grating lines are parallel to the entrance plate reference edge along the X direction within of $\pm 1^\circ$. Their size is a square with dimensions X*Y of 250×250 mm². The total VPHG thickness shall be $50 -0.2/+0.3$ mm. The maximum total wedge for the whole VPHG shall be less than ± 1 arcmin in any direction. It is made of fused silica. Each VPHG should comply with the absolute minimal transmission for first order efficiency requirement over the clear aperture average for the nominal angle of incidence (Blue=50%; Green=70% and Red=70%). The overall diffracted wavefront of VPHG comes from optical surfaces themselves, their coating, the holographic gelatin and bounding process. The overall diffracted wavefront error shall be flat with a maximum power term of ± 20 fringes @ $\lambda=633$ nm. The remaining wavefront irregularities (power removed) shall be less than 4λ PTV / 0.8λ rms at 633nm, over clear aperture.

The VPHG is mounted in a common mount “dispersive assembly”. For the VPHG, only θ_z alignment is identified in the global alignment Table 2.

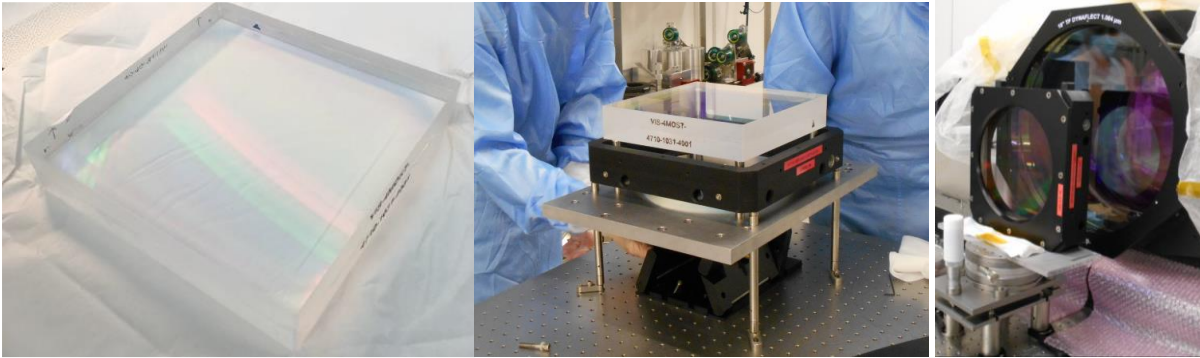


Figure 9: LRS VPHG

4.5 Camera

The cameras consist of three singlets in S-FSL5Y, PBM2Y and S-FSL5Y acting as camera group and manufactured by Winlight System. It has aspheric surfaces on the concave (rear) surface of the second lens and the convex (rear) surface of the third lens. The largest clear aperture is 260 mm which will require a diameter of about 290 mm for this lens if one includes the material needed for mounting and some margins for alignment. The global transmission Blue/Green/Red shall be higher than 89/90/92% in average. Additionally to the camera, a silica singlet acts as Field Lens Window for Detector Vessel. This Field Lens is not mechanical part of the camera but it is an optical one. For the three arms, all camera lenses are identical in terms of curvature, apertures, thicknesses and asphere coefficients. Only air thicknesses are different. All FLW are identical.

The image quality is specified for the {Camera + FLW} in 3 different configurations. The first one, the wavefront error for all lens surfaces on the camera is measured and shall be lower than 40 nm RMS. The second one, a test setup on axis including a FLW will enable the cameras validation before delivery. It is expected to have 80% of ensquared energy in 15 microns². The last verification consists in introducing the measured data in the complete LRS Zemax model to check the degradation of 20% of the spot radius.

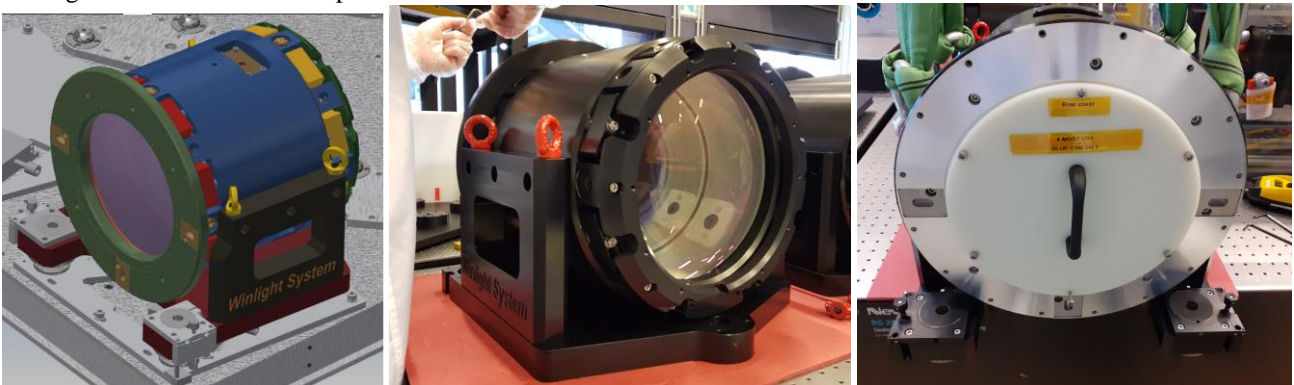


Figure 10: LRS Camera: Design and manufacturing

As the Field Lens is not mechanical part of the camera but it is only an optical one, stringent tolerances are set on the all interfaces (± 0.05 mm in position; ± 0.5 arcmin in orientation).

As previously mentioned the Camera + DV Interface Support will be adjustable in ΘX . In order to complete the necessary alignment degrees of freedom identified in Table 2, a ΘY adjustment is also needed and fitted into the Camera Support at the level of the 2 rear kinematic points. These two X adjustments will be set together in parallel to have pure ΘY rotation at the level of the first kinematic point.

5. MECHANICAL COMPONENTS MANUFACTURING

5.1 Entrance Slit Unit Interface

The LRS Entrance Slit Unit (ESU) houses the end of the science fibres that transmit light from the VISTA focal plane into the LRS. In order to achieve modularity, the 812 science fibres are grouped into 28 slitlets of 29 each. The fibre core diameter is 85 microns positioned in V-groove with a distance between fibre centres in a slitlet of $170\mu\text{m}$. The entrance focal surface of the LRS follows a sphere of 635.61 ± 1 mm radius which is provided by the inner surface of the Slit Lens. Each individual slitlet is positioned against and interfaced with optical gel. An ESU description is presented in the paper [9]. The mechanical support and the cover have been manufactured by DMI, Fr. The remaining parts and integration have been done by Potsdam who is responsible for ESU.

The LRS Fibre is a crucial interface where:

- The Fibre Feed interface is the reference for LRS optical alignment. That is mounted onto a kinematic mount (trihedral point/line/plane system) enabling the mounting and remounting of Entrance Slit Unit in operation in the unlikely and exceptional case where LRS dismounting from the telescope would be required.
- It is mounted on a focusing stage enabling the setting of the correct focus of the slit with regards to the collimator.
- The Entrance Slit Unit is fitted with a shutter mechanism and back illumination system.
- The exit fibers should be referenced wrt its kinematic interface to a tight tolerance enabling interchangeability between tool used for MAIT at CRAL and final unit – given by the table below.

	$\pm X$ (mm)	$\pm Y$ (mm)	$\pm Z$ (mm)	$\pm\theta x$ (arcmin)	$\pm\theta y$ (arcmin)	$\pm\theta z$ (arcmin)
Absolute Tolerance of Fibres wrt ESU mechanical interface	0.2	0.15	0.15	15	15	Derived from Y
Relative Tolerance of Fibres wrt ESU mechanical interface	0.1	0.05	0.02	5	5	Derived from Y

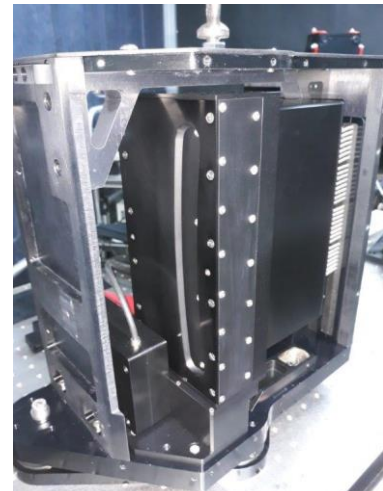
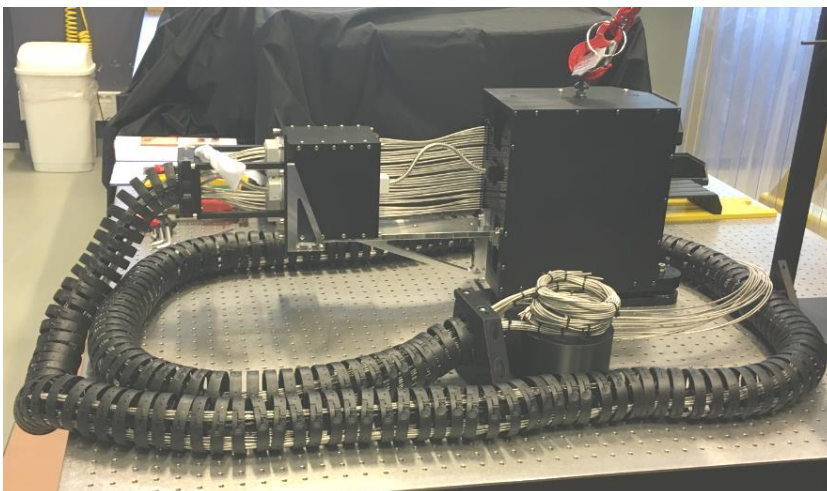


Figure 11: LRS ESU Tool delivered by AIP for the MAIT at CRAL.

5.2 Optical Bench

The purpose of the optical bench main structure is to provide a very stable opto-mechanical reference and mechanical support to all optical components. It has therefore to be very precise in term of flatness and referenced position as well as very stiff to minimize the load deformation. It shall also survive earthquake without permanent deformation. It has been manufactured by Socromo, Fr. The main characteristics of LRS optical bench structure are:

- Full aluminium (7075) 3 parts sandwich type assembly
- 2 plates of 10 mm
- A stiffening structure of 80 mm thickness. The stiffening structure is expected to be realized in water jet cutting. The stiffening structure shape has been opening in FEA to provide a maximum rigidity for a minimum weight.
- It includes a dedicated opening in the lower part of the collimator to optimize the elevation of optical axis
- All fastening threads will include stainless steel inserts for greater resistance and duration.
- The interface between LRS and telescope frame is performed with 3 insulated feet to avoid structure warp and reduce thermal conduction.
- Manufacturing tolerances are expected to be of 0.2 mm in planarity and ± 0.2 mm X, Z.

The positioning and tolerancing is foreseen at the optical bench level. This level shall also ensure proper re-positioning by kinematic mount (manufactured by Almeras, Fr). This is done first, by having the different kinematic mount components mounted on an interface plate. These plates are precisely located and oriented with regards to the optical bench by the mean of 3 pins located in the bench and 3 associated 90° slots located in the interface plate - Figure 12. The pin positioning with regards to one another is expected to be of ± 0.1 mm. Kinematic mount reference surfaces are then precisely or possibly directly machined in the interface plate. This interface plate or components of the kinematic mounts can be shimmed or re-machined in case non-compliance. A repeatability of ± 5 μ m in X, Y, Z for each contact can be assumed in a first step.

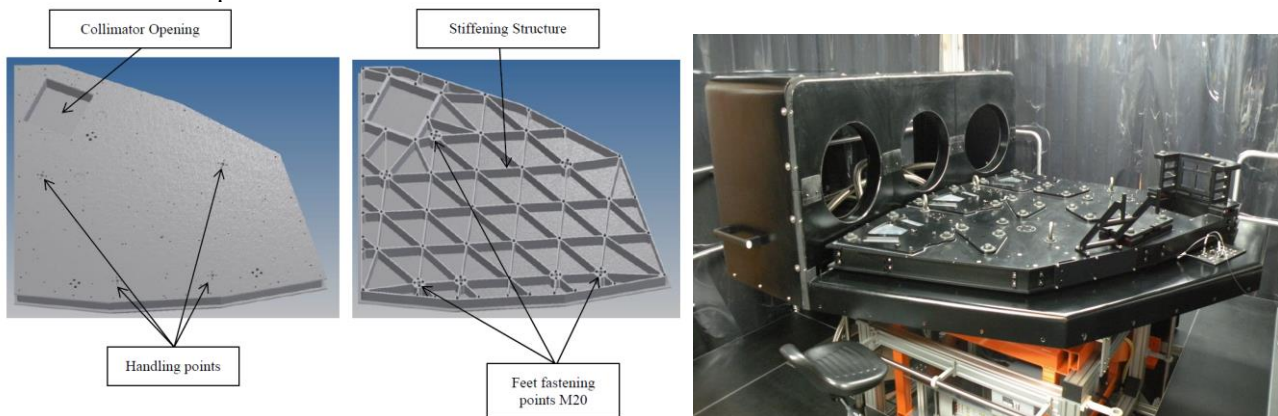


Figure 12: Left: LRS Optical Bench (Top view with and without top plate). Right: LRS Optical Bench with kinematic mounts and cover partially mounted

5.3 Cover

The LRS cover is composed of panels made of fiber glass epoxy (or polyurethane/polyester resin) and polyurethane foam for insulation. The covers have been manufactured by Magma Composites, Fr. The different panels are assembled in three main components which are Top, Lower and DV Cover - Figure 13. Two doors are available for the maintenance: one for DV access and the other one for the Entrance Slit Unit installation on the telescope and for the shutter motor maintenance. The LRS will be heated with some conducting heating foil. For better heat radiative homogeneity, these foils will be glued on 8 blacked aluminum plate inside the covers. With EPDM foam sealing and labyrinth shape edges, the overall tightness inside the main optical volume is expected to be very good for light tightness and close to gas tightness. Moreover, it will be flowed through the DV with clean dry nitrogen providing possibly a small overpressure. The LRS is therefore expected to be perfectly light tight and dust tight.

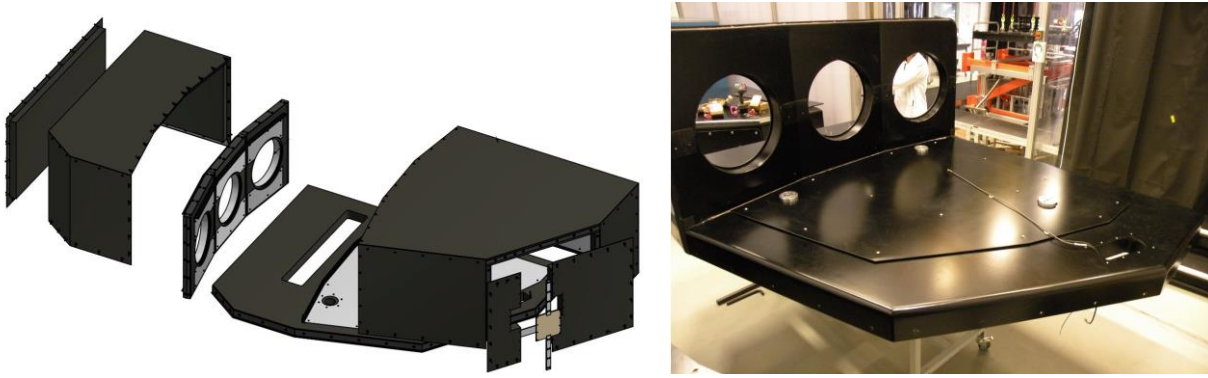


Figure 13: LRS Cover: Design and manufacturing

5.4 Detector Interface Assembly

As shown in the global alignment Table 2, (z , θ_x , θ_y) adjustment on the DV is foreseen. This function is ensured by the Detector Interface Assembly presented in Figure 14 and manufactured by Lucchese, Fr. That is done by the mean of 3 taped pistons, synchronized and controlled by a common motorized gear ring. The whole focusing system even if very stable because of a negligible backlash in the gear mount is nevertheless completely fastened after setting by the mean of controlled passive clamping actuator.

It is to be noted that the focus alignment is the only adjustment that can be used after installation of the LRS on the telescope without opening the LRS. Though it is though mainly as an initial alignment device, it will possible to refocus one or several arms in case of exceptional earthquake or unexpected event. As the LRS is thermally controlled, regular or seasonal refocusing is not required. The θ_X and θ_Y adjustments are done by the mean of 2 wedges sliding together during the MAIT phase only.

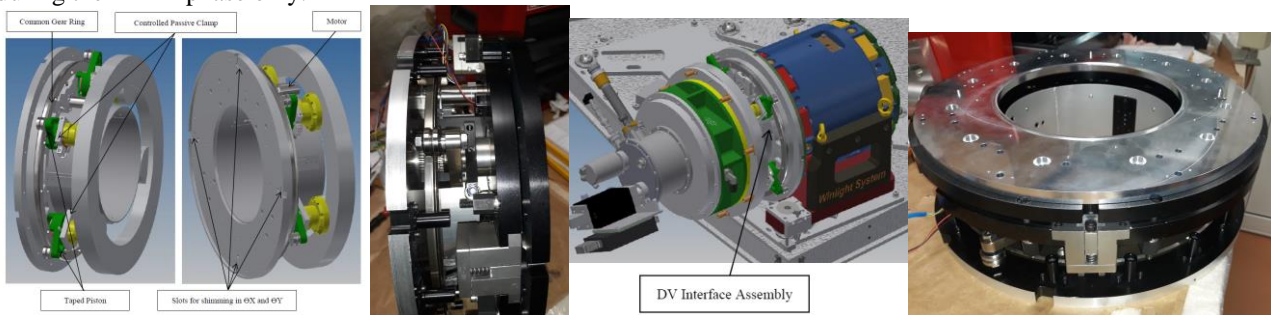


Figure 14: LRS Detector Interface Assembly: Design and manufacturing

5.5 Detector Interface

The LRS Detector System mechanical interface is mostly at the level of the LRS Camera-DV interface. As shown below, this interface enables the proper positioning of the DV as a whole including the CCD but also the proper positioning of the Field Lens Window. The Field Lens is particularly tricky as it is optically speaking part of the camera but mechanically speaking part of the DV. Both assemblies are therefore precisely positioning with regards to the same interface flange surface. This is achieved by a set of 3 pins mounted in the camera and the Field Lens Window assembly and 2 times 3 associated slots at 90° in the DV - Figure 15. ESO is responsible for the manufacturing.

	$\pm X$ (mm)	$\pm Y$ (mm)	$\pm Z$ (mm)	$\pm \theta_x$ (arcmin)	$\pm \theta_y$ (arcmin)	$\pm \theta_z$ (arcmin)
Position of FLW wrt DV mechanical interface	0.01	0.01	0.01	0.5	0.5	0.5
Position of CCD wrt DV mechanical interface	0.075	0.075	0.05	0.5	0.5	2
Position of Camera Interface wrt Camera mechanical interface	0.07	0.07	0.05	2.5	2	2.5

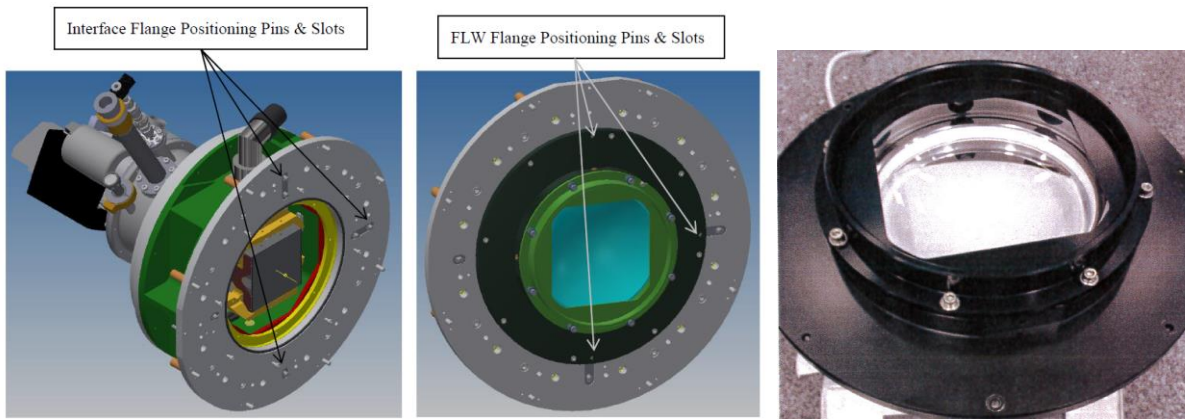


Figure 15: Left: DV. Middle: Camera-DV Interface and FLW interface; Right: FLW

6. CONCLUSION AND FUTURE DEVELOPMENT

During this MAIT phase, all optical and mechanical components have been ordered with stringent tolerances in order to fulfil top-level requirements. A MAIT plan for 4MOST LRS in Lyon Integration Hall has been proposed to allow to assess a compliance with requirements and an integration in safe conditions. Currently, 90% of the orders have been delivered at CRAL. For LRS-A, the integration is on-going. The step_1 (optical bench correctly aligned to start optical alignment) and step_2 (alignment of fibres, collimator and dichroics) are finished. The first results are very encouraging. We plan to perform the first exposures early in January, 2021. At this date, the integration of LRS-B could start in parallel. We expect a Local Acceptance Review for LRS-A in September, 2021 and November, 2021 for LRS-B. There is then a good hope that the finally build LRS instrument will match its ambitious scientific performances.

I finally would like to particularly thank the members of the 4MOST CRAL team, AIP Project Office members and everyone working on 4MOST project for their support and invaluable contribution to this encouraging 4MOST LRS MAIT phase.

We acknowledge the financial support of CRAL, CNRS/INSU, Université de Lyon, Université Claude-Bernard Lyon1 and the Labex Lyon Institut of Origin (LIO).

REFERENCES

- [1] Roelof de Jong et al., " 4MOST: the 4-metre Multi-Object Spectroscopic Telescope project status: instrument manufacturing and integration, operations development, and survey planning," Proc SPIE 11447-238 (2020)
- [2] Nicolas Azais et al., " Wide-field corrector for 4MOST: design details and MAIV processes," Proc SPIE 9908, 308 (2016)
- [3] Jurek Brzeski et al., " AESOP: The 4MOST fibre positioner," Proc SPIE 11447-201 (2020)
- [4] Walter Seifert et al., " 4MOST: MAIT of the High-Resolution-Spectrograph," Proc SPIE 11447, 211 (2020)
- [5] Jakob C. Walcher et al., " 4MOST: science operations for a large spectroscopic survey program with multiple science cases executed in parallel," Proc SPIE 9910, 69 (2016)
- [6] Steffen Frey et al., "4MOST preliminary instrument design," Proc SPIE 9908, 310 (2016)
- [7] Olga Bellido-Tirado et al., " 4MOST systems engineering: from conceptual design to preliminary design review," Proc SPIE 9911, 76 (2016)
- [8] Eléonore Barthélémy-Mazot et al., " Dichroic coatings for astronomical instrumentation," Proc SPIE 11451, 189 (2020)
- [9] Andreas Kelz et al., " 4MOST fiber system: MAIT of the test-slit-units," Proc SPIE 11447, 218 (2020)